frontiers | Frontiers in Earth Science

ORIGINAL RESEARCH
published: 09 June 2022
doi: 10.3389/feart.2022.865575

# Carbon Isotope Composition and Geochemical Features of Sediments From Gongga Mountain, China, and Potential Environmental Implications

*Yingqin Wu*[1*†], *Tong Wang*[2,3†], *Yan Liu*[1], *Rong Ma*[1,4] *and Zhangxin Chen*[5*]

[1]Key Laboratory of Petroleum Resources, Gansu Province/Northwest Institute of Eco-Environment and Resources, Chinese Academy of Sciences, Lanzhou, China, [2]School of Environment, Beijing Jiaotong University, Beijing, China, [3]School of Engineering, Newcastle University, Newcastle, United Kingdom, [4]University of Chinese Academy of Sciences, Beijing, China, [5]Department of Chemical and Petroleum Engineering, Schulich School of Engineering, University of Calgary, Calgary, AB, Canada

OPEN ACCESS

**Edited by:**
Zhang Chengjun,
Lanzhou University, China

**Reviewed by:**
Yufeng Jiang,
Lanzhou Jiaotong University, China
Jianfa Chen,
China University of Petroleum, China

***Correspondence:**
Yingqin Wu
yingqinwu@lzb.ac.cn
Zhangxin Chen
zhachen@ucalgary.ca

†These authors have contributed equally to this work and share first authorship

**Specialty section:**
This article was submitted to Geochemistry,
a section of the journal
Frontiers in Earth Science

**Received:** 30 January 2022
**Accepted:** 19 May 2022
**Published:** 09 June 2022

**Citation:**
Wu Y, Wang T, Liu Y, Ma R and Chen Z (2022) Carbon Isotope Composition and Geochemical Features of Sediments From Gongga Mountain, China, and Potential Environmental Implications. Front. Earth Sci. 10:865575. doi: 10.3389/feart.2022.865575

Using gas chromatography-triple quadrupole tandem mass spectrometry (GC-MS/MS), the soluble organic matter was analyzed for the first time in twenty-two sediment samples from the eastern slopes of the Gongga Mountain, China, at high altitudes between 4,600 and 6,700 m. The $C_{11}$-$C_{33}$ *n*-alkanes and $C_9$-$C_{33}$ *n*-alkan-2-ones were identified in these samples. Both compounds were dominated by odd carbon numbers in the long-chain molecules and contained a maximum of *n*-$C_{27}$ or *n*-$C_{29}$, indicating that the sediments were predominantly of higher plant origin. However, the short-chain *n*-alkan-2-ones, with a maximum content of *n*-$C_{17}$ or *i*-$C_{18}$ (phytone, 6, 10, 14-trimethylpentadecan-2-one), did not show a predominance of odd and even numbers, suggesting that they were predominantly derived from bacteria and algae. Therefore, we suggest that the organic matter in Gongga Mountain comes from three sources, i.e. bacteria, algae, and higher plants. Stable carbon isotope ($\delta^{13}C$) values ranged from –24.6‰ to –27.3‰, indicating that $C_3$ plants were the dominant organic input to the sediments and suggesting a relatively colder and drier depositional environment. However, $C_4$ plants increase sharply at high altitudes of 6,300–6,600 m, suggesting that the paleoclimate of Gongga Mountain became drier and wetter with the increase of altitude.

**Keywords: *n*-alkanes, *n*-alkan-2-ones, geochemical features, carbon isotope composition, Gongga Mountain**

## INTRODUCTION

*N*-alkanes and *n*-alkan-2-ones are abundant in almost all plants and can account for more than 60% of the epidermal lipids. Both of these organic compounds are relatively resistant to degradation after plant decay (Poynter and Eglinton, 1991). These components can show signals of their presence in the sediments (Jansen et al., 2008). Thus, the *n*-alkanes and *n*-alkan-2-ones can be particularly useful as biomarkers for understanding the source of organic matter, and for tracking ecosystem changes and reconstructing palaeo-vegetation (Nichols and Huang., 2007; Andreou and Rapsomanikis 2009; Badewien et al., 2015; Li G. et al., 2018). For example, some indexes of long-chain *n*-alkanes reflect the relative proportion of lower organisms such as bacteria, algae, and higher plants (Crausbay et al., 2014; Wang et al., 2014; Bush and McInerney 2015; Howard et al., 2018). These indexes include the *n*-alkane average chain length (ACL), the ratios of trees to grasses (*n*-$C_{29}$/*n*-$C_{31}$), the ratios of $\sum n$-$C_{21-}$/$\sum n$-$C_{21+}$ in *n*-alkanes and a carbon preference index (CPI). In addition, the organic carbon isotope values ($\delta^{13}C$) can be used to estimate the relative contributions of $C_3$ and $C_4$ plants, infer paleoclimate changes, and to examine past primary productivity (France-Lanord and Derry 1994). Consequently, we analyzed the biomarkers and the organic carbon isotope values ($\delta^{13}C$) of surface sedimens along an elevation transect on the eastern slope of Gongga Mountain, ranging in elevation from 4,600 m to 6,700 m.

Some soil biomarkers may be useful tools for palaeo-vegetation reconstruction (Didyk et al., 1978; Bai et al., 2020). And while some relevant biomarker studies have previously been done on low elevation soil samples from the Gongga Mountains (Jia et al., 2008; Bezabih et al., 2011; Bai et al., 2011; 2020), the studies on high elevation sediment samples are currently lacking. The reason for this may be due to the fact that sampling becomes much more difficult as the altitude increases. Our study aimed to identify and understand the geochemical characteristics of high-altitude ecosystems in the Gongga Mountain and to reconstruct the local palaeo-vegetatio and track ecosystem changes by measuring the carbon isotope composition and lipid biomarkers in the sediments. Furthermore, in this study, we used lipid biomarkers and $\delta^{13}C$ analyses to determine how the lipid biomarkers and carbon isotopes can be used to delineate the source of organic matter and related processes.

## SAMPLING AREA, SAMPLES AND METHODS

### Sampling Area and Samples

Gongga Mountain, is the highest peak (7,556 m a.s.l) in the Hengduan Mountains. It is located approximately 30°N and 102°E in the middle and southern section of the Big Snow Mountain Range and on the southeastern edge of the Tibetan Plateau in Sichuan Province, southwest China. It is a unique mountain in western China because it contains both modern low-latitude glacial features and an integrated vertical vegetation distribution ranging from subtropical forests to tundra. Compared with other mountain ranges in China, before the Gongga Mountain, the Gongga Mountain range still has an extensive area of primary coniferous and deciduous forests to an elevation of 4,000 m. With a vertical range of more than 6,300 m along only 11 km of horizontal distance, the eastward slope drops towards the Sichuan Basin in southwestern China. The mean annual temperature is 4°C. The annual rainfall is approximately 1938 mm, and 85% of the rainfall falls during May to October, according to the meteorological station located 3,000 m above sea level (a.s.l) (Alpine Ecosystem Observation and Experiment Station of Gongga Mountain, Chinese Academic of Sciences). The regional climate is characterized by typical monsoon patterns of temperature, precipitation, and evaporation. This region is influenced by both the Pacific and the Indian Ocean meteorological systems, which bring southeasterly and southwesterly monsoons, respectively. There are many special characteristics of the mountain ecosystem and environment in the Gongga Mountain Region, including tropical and subtropical cold-loving plant species (Luo et al., 2015). The hottest months occur well within the rainy season, from May to September, while evaporation peaks during the

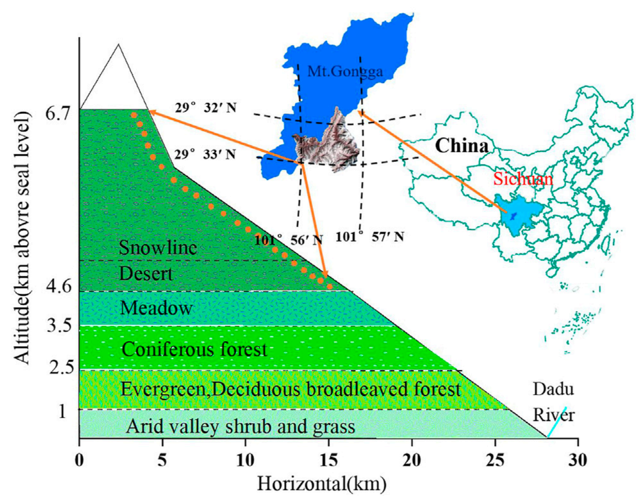


**FIGURE 1 |** The vertical vegetation zonation and climatic conditions on the eastern slope of Gongga Mountain, according to Zhong et al. (1999), Thomas (1997) and Jia et al. (2008).

sunny, pre-monsoon months (Thomas 1997, 1999). The eastern slope of Gongga Mountain, which is the transitional zone of the first and second step in China, has disparate plant ecosystems at different elevations (Thomas 1999; Zhong et al., 1999). Gongga Mountain is therefore an area with very high biodiversity: approximately 2,500 plant species belonging to 869 genera and 185 families have been identified in this region (Thomas 1999). However, the plant species at high elevations (above the snowline) have not been reported. As a result, selected study area is 4,600–6,700 m above sea level in a typical ecosystem of Gongga Mountain east of the Tibetan Plateau (**Figure 1**). In June 2012, 22 surface sediment samples (5–10 cm above ground level) were collected from the eastern slope of the Gongga Mountain by removing the layers of snow, ice and litter. The samples were collected over a period of 2 weeks. The altitude of each sampling site was determined by using a GPS unit with an error of ±10 m. Samples at each location were taken from three sub-samples that were evenly mixed and bagged. These three sampling locations were collected randomly within an approximate 10 m radius using an electric drill and metal shovel. All samples were wet, and each of them was tightly sealed on site in polyethylene zipper bags. The first bag was sealed in a second, "outer," zipper bag to insure against possible damage and leakage. Bagged samples were frozen immediately after transit to the laboratory.

### Analytical Methods

All sediment samples were dried at room temperature and crushed to 100 mesh. Powders were kept frozen at about −18°C until analysis. An aliquot (~250 g) of each sample was Soxhlet-extracted with a mixture of dichloromethane-methanol (93:7, v/v) for 72 h, and then the extracts were separated into saturate, aromatic and polar fractions by a glass chromatographic column packed with activated silica gel and eluted by solvents of increasing polarity. The details of the extraction and separation have been published elsewhere (Wu et al., 2016). The fractions obtained were analyzed using the full scan and the selected ion monitoring (SIM) modes.

**TABLE 1** | Results of TOC/$\delta^{13}C$(‰) analysis and calculated parameters of samples at Gongga Mountain.

| Sample# | Altitude (m) | TOC (%) | $\delta^{13}C$(‰) (Das) |
|---|---|---|---|
| GGS-1 | 6,700 | 2.57 | –25.2 |
| GGS-2 | 6,600 | 2.13 | –24.6 |
| GGS-3 | 6,500 | 2.30 | –24.4 |
| GGS-4 | 6,400 | 2.08 | –24.7 |
| GGS-5 | 6,300 | 3.05 | –24.7 |
| GGS-6 | 6,200 | 3.11 | –25.1 |
| GGS-7 | 6,100 | 1.34 | –25.4 |
| GGS-8 | 6,000 | 2.57 | –25.0 |
| GGS-9 | 5,900 | 2.06 | –25.2 |
| GGS-10 | 5,800 | 1.46 | –24.8 |
| GGS-11 | 5,700 | 2.65 | –25.4 |
| GGS-12 | 5,600 | 3.23 | –25.8 |
| GGS-13 | 5,500 | 3.35 | –26.2 |
| GGS-14 | 5,400 | 3.85 | –25.5 |
| GGS-15 | 5,300 | 4.59 | –26.1 |
| GGS-16 | 5,200 | 3.91 | –26.4 |
| GGS-17 | 5,100 | 5.21 | –26.0 |
| GGS-18 | 5,000 | 2.68 | –25.8 |
| GGS-19 | 4,900 | 2.87 | –25.9 |
| GGS-20 | 4,800 | 3.59 | –25.1 |
| GGS-21 | 4,700 | 3.30 | –27.3 |
| GGS-22 | 4,600 | 3.77 | –26.1 |

*TOC, total organic carbon.*

A GC-MS/MS analysis was performed using a Hewlett-Packard 7890 gas chromatograph (GC) coupled to a Hewlett-Packard 7000B mass selective detector (MSD). The GC was fitted with a HP-5 capillary column (30 m × 0.25 mm×0.25 μm, Agilent, United States), based on a previous study (Wu et al., 2016). The oven temperature was initially 80°C (1 min) and was then increased to 290°C at a rate of 4°C/min and finally held at this temperature for 30 min. Helium was used as the carrier gas at a linear velocity of 28 cm/s, with a GC inlet temperature of 300°C and the injector operating at a flow rate of 0.9 ml/min. The MSD was operated with an ionization energy of 70 eV and a source temperature of 230°C. Data were collected in full-scan mode and scanned from 10 to 550 amu.

Organic carbon isotope analyses are carried out at Oil and Gas Research Center, Northwest Institute of Eco-Environment and Resources (Chinese Academy of Sciences). Firstly, dilute hydrochloric acid was added to sediment sample to remove inorganic carbon, and then the decarbonated and dried sediment sample was analyzed using a Thermo Fisher MAT 253-Flash2000 mass spectrometer. Calibration measurements were performed using a standard reference IAEA-600 ($\delta^{13}C$ = −27.77‰), with calculated standard deviations of less than 0.2‰ per 6 measurements resulting in $\delta^{13}$Corg (Coplen et al., 2006).

## RESULTS

### Total Organic Carbon Content and Its Isotopes

The TOC contents of the samples range from 1.34 to 5.21% with an average value of 2.99% (**Table 1**). In addition, the TOC content showed a systematic variation with elevation, peaking in sediments from an elevation of 5,100 m (**Table 1**). The $\delta^{13}C$ values range from −24.4‰ to −27.3‰ (**Table 1**), indicating that $C_3$ plants were dominant along the eastern slope of Gongga Mountain (Wei et al., 2015).

### Distribution of Aliphatic Hydrocarbons and Alkanones

The distributions of *n*-alkanes and *n*-alkan-2-ones were measured by mass chromatography of the fragment ions m/z 85 (**Figure 2**) and m/z 58 (**Figure 3**). These compounds were identified by comparison of measured mass spectral data and retention indices to published data (George and Jardine 1994; Wu et al., 2012). The aliphatic hydrocarbon fraction consists mainly of *n*-alkanes and isoprenoid alkanes (pristane (Pr) and phytane (Ph)). Straight-chain alkanes are the most abundant hydrocarbons in the extracts (**Figure 2**). The *n*-alkanes are in the $C_{11}$ to $C_{33}$ range, with peaks of *n*-$C_{27}$ or *n*-$C_{29,}$ and the sediment samples studied show a uni-modal characteristic distribution. The odd over even carbon number predominance ($OEP_{27}$) is significantly greater than 1.0 for all samples, ranging from 3.29 to 6.27. The carbon preference index ($CPI_{25-31}$) ranges from 3.33 to 6.49, and the average chain length (ACL) ranges from 27.37 to 28.33. In samples from elevations of 4,700 m, 5,400 m, 5,800 m, 5,900 m, 6,600 m, and 6,700 m, the Pr content is higher than the Ph content, and the Pr/Ph ratios range from 1.09 to 1.51. However, in other samples, the Ph content is slightly higher than the Pr content, and the Pr/Ph ratios range from 0.66 to 0.94 (**Table 2** and **Figure 4**).

The *n*-alkan-2-ones range from $C_9$ to $C_{33}$ and are characterized by bi-modal distributions with a higher relative abundance of the higher-molecular-weight (HMW) homologues, dominated by $C_{27}$ or $C_{29}$, and lower amount of short chain *n*-Alkan-2-ones, dominated by *n*-$C_{17}$ or *i*-$C_{18}$ (phytone, 6,10,14-trimethylpentadecan-2-one). The short chain components show no strong odd/even carbon number preference; however, the long chain components range from *n*-$C_{23}$ to *n*-$C_{33}$, with a strong odd/even preference.

## DISCUSSIONS

### Vegetation Composition of the Study Area and Depositional Conditions

The $\delta^{13}C$ values of TOC in soils and sediments reflect the changes of $C_4$/$C_3$ plant input ratios (France-Lanord and Derry 1994; Cayet and Lichtfouse, 2001; Badewien et al., 2015). Typically, $C_3$ plants have $\delta^{13}C$ values ranging from −20% to −32%, whereas $C_4$ plants have $\delta^{13}C$ values from −9% to −17% (Denies, 1980; Farquhar et al., 1989; Sukumar et al., 1993; Lim et al., 2010; Sun et al., 2012). Yang, (2012) suggested that lower temperature and reduced summer precipitation favoured $C_3$ over $C_4$ plant, i.e. $C_3$ plants dominated in cooler and drier conditions, whereas $C_4$ plants favoured warmer and wetter climates. To investigate the paleoclimates and paleoenvironments on the east side of the Tibetan Plateau, Southwest China, the $\delta^{13}C$ values of the organic matter in sediments were determined for the sediments along the

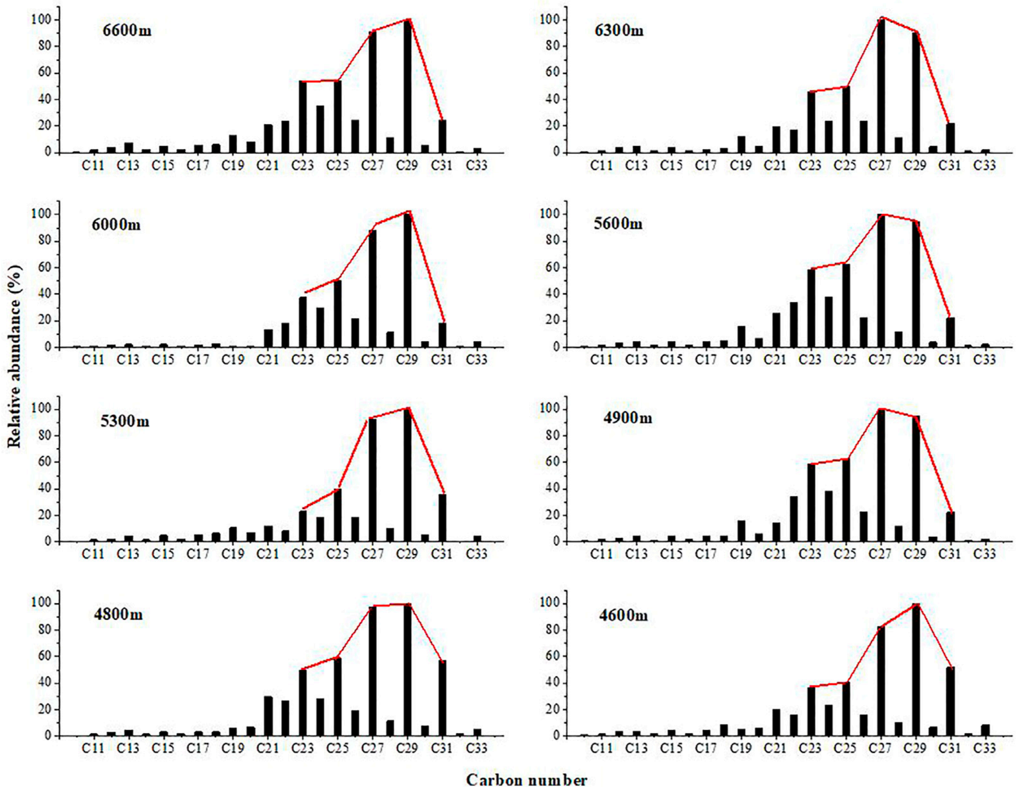


**FIGURE 2 |** Distributions of *n*-alkane in the sediment samples from Gongga Mountain.

eastern slope of Gongga Mountain. As shown in **Table 1** and **Figure 4**, these values range from −24.6‰ to −27.4‰; the lower-altitude sediments had lower $\delta^{13}C$ values, while sediments from 6,300–6,600 m had higher $\delta^{13}C$ values of −24.7‰, −24.7‰, −24.4‰ and −24.6‰, respectively. These results indicate that $C_3$ plants were likely important contributors to organic compounds in the sediments. Therefore, in general, the climate was probably cold and dry along the eastern slope of Gongga Mountain. The results also showed that the lower-altitude sediments had lower $\delta^{13}C$ values, suggesting that the more terrigenous $C_3$ plants dominated at lower altitudes. In addition, the $\delta^{13}C$ values of organic matter in sediments tended to be positive with increasing altitude. From this phenomenon, we speculated whether some amount of $C_4$ plants could have been present. If $C_4$ plants are present, then a temporary warming and wetting of the palaeoclimate at 6,300–6,600 m may have occurred. (Sukumar et al., 1993; Liu et al., 2005; Xue et al., 2014). However, its cause needs to be further investigated.

The *n*-alkanes were dominated by *n*-$C_{27}$ or *n*-$C_{29}$ with a single peak distribution (**Figure 2**). $OEP_{27}$ was significantly greater than 1.0 for all samples (ranging between 3.29 and 6.27). Furthermore, at 4,600, 4,800, 5,200, and 5,500 m, the distribution of *n*-alkanes in the sediments showed a clear odd-numbered dominance, suggesting a dominant contribution from higher plants, but also a small input of algae (Lichtfous et al., 1994). In addition, no significant correlation was found between the Pr/Ph ratio and altitude. In samples from elevations of 4,700, 5,400, 5,800, 5,900, 6,600 and 6,700 m, the Pr/Ph ratios range from 1.09 to 1.51, indicating weakly oxic depositional conditions. However, in other samples, the Ph content is slightly higher than the Pr content, and the Pr/Ph ratios range from 0.66 to 0.94 (**Table 2** and **Figure 4**). These results are indicative of a suboxic reductive environment (Hughes, Holba, and Dzou. 1995; Rontani et al., 2013).

## Relationship Between $\delta^{13}C$ Values and Altitude, Temperature and Humidity

The change in $\delta^{13}C$ value of TOC varied between −24.6‰ and −27.3‰from 4,700 m to 6,700 m above sea level on the eastern slope of Gongga Mountain (**Table 1**). Linear regression analysis showed that $\delta^{13}C$ values of sediments were positively correlated with altitude (**Figure 5**). The changes in $\delta^{13}C$ value and altitude were characterized by an abrupt fall from 4,600 to 4,700 m, followed by an abrupt increase at 4,800 m. Then, the values were rather stable between 4,900 m and 6,200 m, followed by an moderate increase from 6,300 m to 6,600 m (**Figure 4**, **5**).

The stable carbon isotope values ($\delta^{13}C$) of sediments in Gongga Mountain ranged from −24.6‰ to −27.3‰, indicating that $C_3$ plants were the main organic inputs to the sediments (Vogts et al., 2009). The increase in $C_3$ plants from low altitude to high altitude in Gongga Mountain was suggested to reflect the influence of decreasing temperature. Thus, the general trend showed a relatively drier and colder sedimentary environment

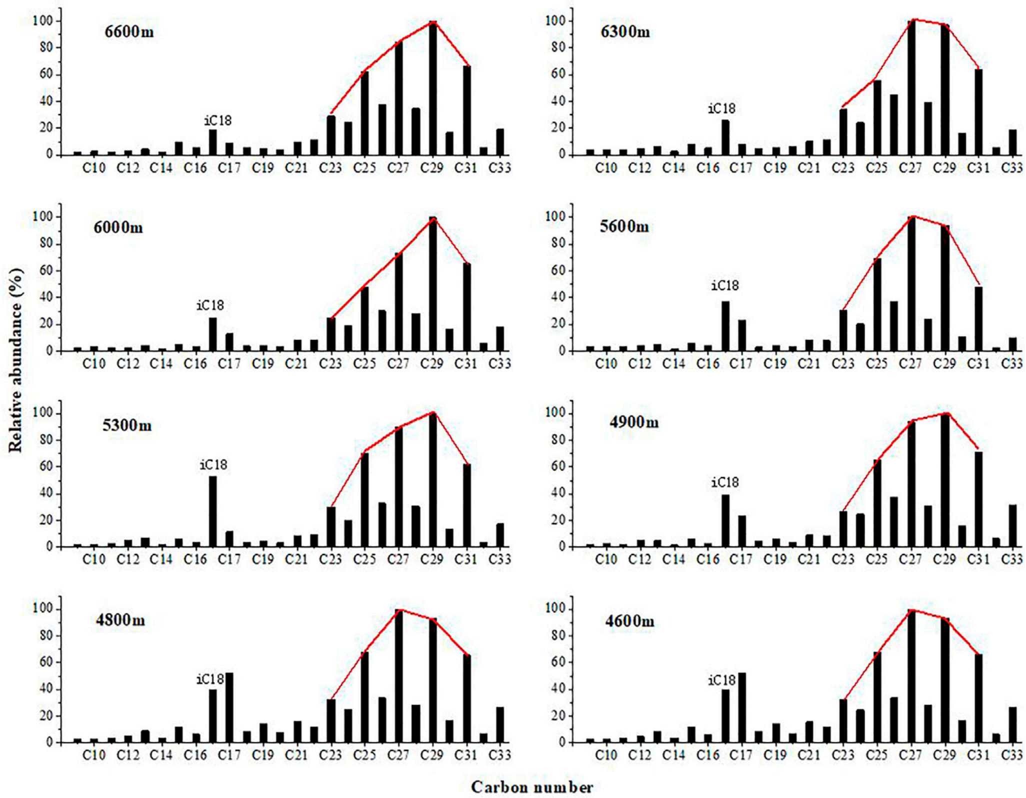


**FIGURE 3 |** Distributions of *n*-alkane-2-ones in the sediment samples from Gongga Mountain.

with the increase of altitude. However, there was a sharp increase of $C_4$ plants from 4,700 m to 4,800 m, and a mild increase of $C_4$ plants from 6,300 m to 6,600 m. This phenomenon reflected that there may be a temporary warming trend in the altitude range of 4,700 m to 4,800 m and 6,300 m to 6,600 m. The cause of this phenomenon need to be considered in future studies.

## Molecular Abundance, Distribution, Origin and Potential Significance of *n*-Alkanes

*n*-Alkanes are widely present in plants and other organisms. The source of organic matter can be traced through the distribution characteristics of *n*-alkanes because different biological sources of *n*-alkanes possess different distribution characteristics. Previous studies showed that *n*-alkanes from lower organisms range from $n$-$C_{15}$ to $n$-$C_{20}$, often with $n$-$C_{17}$ or $n$-$C_{19}$ as the dominant compounds and without an obvious odd-over-even preference (Eglinton and Hamilton 1967). In contrast, long-chain *n*-alkanes are mostly derived from epicuticular waxes of leaves from vascular higher plants (Meyers 1997; Fang et al., 2014; Cortina et al., 2016). In addition, woody plants display *n*-alkane distributions dominated by $C_{27}$ or $C_{29}$ *n*-alkanes, whereas grasses produce distributions dominated by the $C_{31}$ *n*-alkane (Li et al., 2016). Hence, *n*-alkane distribution patterns can be used to estimate changes in vegetation types (Al-Aklabi et al., 2016). Modern organic geochemistry of molecules shows that the ratio $\sum n$-$C_{21}^{-}/\sum n$-$C_{21}^{+}$ reflects the proportion of lower organisms, such as bacteria and algae relative to higher plants (Li G. et al., 2018). In this study, the *n*-alkane carbon numbers range from $C_{11}$ to $C_{33}$ with maxima at $n$-$C_{23}$ to $n$-$C_{31}$ (**Figure 2**) and exhibit a unimodal distribution. The main peaks of unimodal distribution are at $n$-$C_{27}$ or $n$-$C_{29}$, and the long-chain *n*-alkanes had odd-carbon-number predominance, indicating that they were mainly derived from terrestrial higher plants. As shown in **Table 2**, the ratio $\sum n$-$C_{21}^{-}/\sum n$-$C_{21}^{+}$ ranged from 0.07 to 0.29 (average 0.64), also suggesting that higher plants were the main source of organic matter to sediments at elevations from 4,600 m to 6,400 m.

The *n*-alkane CPI in sediment is also an indicator of the sources of organic matter (Collister et al., 1994; Routh et al., 2014). Hydrocarbons composed of a mixture of compounds originating from land plant material show a predominance of odd-numbered carbon chains with CPI = 5–10 (Eglinton and Hamilton 1967; Collister et al., 1994; Bi et al., 2005; Duan and Xu 2012), whereas anthropogenic and reworked materials have low CPIs of approximately 1.0 (Bray and Evans 1961; Mille et al., 2007). CPI values close to 1.0 are also thought to indicate a greater input from marine microorganisms and/or recycled organic matter (Bi et al., 2005). High-molecular-weight *n*-alkanes in these sediment samples range from $n$-$C_{23}$ to $n$-$C_{33}$, with the most abundant being $n$-$C_{27}$ and $n$-$C_{29}$. A clear predominance of odd-carbon-number compounds is exhibited, as indicated by the

**TABLE 2 |** Altitude and biomarker parameters of the sediment samples along eastern slope of Gongga Mountain.

| Sample | Altitude (m) | *n*-Alkane | | | | | Isoperiod | | | *n*-alkan-one | | | |
|---|---|---|---|---|---|---|---|---|---|---|---|---|---|
| | | $CPI^{a}_{25–31}$ | $OEP^{b}_{27}$ | $C_{21-}/C_{21+}$ | $C_{29}/C_{31}$ | $ACL^{c}$ | Pr/Ph | Pr/$nC_{17}$ | Ph/$nC_{18}$ | $CPI^{a}_{25–31}$ | $OEP^{b}_{27}$ | $C_{21-}/C_{21+}$ | $C_{29}/C_{31}$ |
| GGS-1 | 6,700 | 4.87 | 4.67 | 0.13 | 4.34 | 27.69 | 1.51 | 0.55 | 0.34 | 2.86 | 3.35 | 0.12 | 1.47 |
| GGS-2 | 6,600 | 5.07 | 4.93 | 0.18 | 4.04 | 27.76 | 1.17 | 0.48 | 0.51 | 3.04 | 3.63 | 0.13 | 1.51 |
| GGS-3 | 6,500 | 4.86 | 4.80 | 0.16 | 3.55 | 27.73 | 0.67 | 0.48 | 0.63 | 2.89 | 3.43 | 0.16 | 1.42 |
| GGS-4 | 6,400 | 5.44 | 5.03 | 0.21 | 3.93 | 27.86 | 0.92 | 0.47 | 0.45 | 3.10 | 3.91 | 0.20 | 1.42 |
| GGS-5 | 6,300 | 5.34 | 5.32 | 0.15 | 4.17 | 27.67 | 0.96 | 0.42 | 0.45 | 2.78 | 3.40 | 0.15 | 1.53 |
| GGS-6 | 6,200 | 5.99 | 5.51 | 0.10 | 3.80 | 27.83 | 0.84 | 0.40 | 0.44 | 3.07 | 3.80 | 0.10 | 1.49 |
| GGS-7 | 6,100 | 3.33 | 3.29 | 0.16 | 4.16 | 27.37 | 0.92 | 0.43 | 0.51 | 2.99 | 3.74 | 0.25 | 1.88 |
| GGS-8 | 6,000 | 5.37 | 5.19 | 0.07 | 5.52 | 27.75 | 0.82 | 0.49 | 0.56 | 3.31 | 4.15 | 0.13 | 1.52 |
| GGS-9 | 5,900 | 5.60 | 5.60 | 0.06 | 4.94 | 27.69 | 1.55 | 0.75 | 0.56 | 3.15 | 3.76 | 0.08 | 1.51 |
| GGS-10 | 5,800 | 4.79 | 4.45 | 0.12 | 4.35 | 27.61 | 1.09 | 0.54 | 0.46 | 3.13 | 3.83 | 0.08 | 1.77 |
| GGS-11 | 5,700 | 4.23 | 3.80 | 0.29 | 3.16 | 27.64 | 0.96 | 0.44 | 0.50 | 3.18 | 4.26 | 0.22 | 1.70 |
| GGS-12 | 5,600 | 5.48 | 5.65 | 0.16 | 4.31 | 27.59 | 0.86 | 0.47 | 0.52 | 3.80 | 5.13 | 0.15 | 1.97 |
| GGS-13 | 5,500 | 6.23 | 6.27 | 0.10 | 3.26 | 27.87 | 0.85 | 0.65 | 0.59 | 3.34 | 4.11 | 0.10 | 1.63 |
| GGS-14 | 5,400 | 4.54 | 4.41 | 0.15 | 3.60 | 27.56 | 1.17 | 0.46 | 0.47 | 3.06 | 3.71 | 0.12 | 1.82 |
| GGS-15 | 5,300 | 6.45 | 6.05 | 0.16 | 2.85 | 28.05 | 0.68 | 0.39 | 0.51 | 3.68 | 4.27 | 0.13 | 1.61 |
| GGS-16 | 5,200 | 6.36 | 6.25 | 0.12 | 2.96 | 27.92 | 0.77 | 0.43 | 0.56 | 3.43 | 4.43 | 0.16 | 1.54 |
| GGS-17 | 5,100 | 5.52 | 5.28 | 0.15 | 2.65 | 27.80 | 0.94 | 0.42 | 0.48 | 3.48 | 4.39 | 0.12 | 1.88 |
| GGS-18 | 5,000 | 5.24 | 5.59 | 0.08 | 2.03 | 27.75 | 0.69 | 0.46 | 0.48 | 3.43 | 4.09 | 0.12 | 1.38 |
| GGS-19 | 4,900 | 5.45 | 5.58 | 0.13 | 4.30 | 27.59 | 0.66 | 0.45 | 0.67 | 3.35 | 4.13 | 0.14 | 1.40 |
| GGS-20 | 4,800 | 6.25 | 6.02 | 0.14 | 1.76 | 28.08 | 0.82 | 0.42 | 0.55 | 3.50 | 4.04 | 0.28 | 1.42 |
| GGS-21 | 4,700 | 5.46 | 4.96 | 0.10 | 2.27 | 28.14 | 1.15 | 0.50 | 0.65 | 3.47 | 4.00 | 0.28 | 1.42 |
| GGS-22 | 4,600 | 6.49 | 6.21 | 0.15 | 1.92 | 28.33 | 0.61 | 0.45 | 0.55 | 3.50 | 4.02 | 0.28 | 1.41 |

[a] $CPI_{25–31} = 0.5\times[(C_{25} + C_{27} + C_{29} + C_{31})/(C_{24} + C_{26} + C_{28} + C_{30})+(C_{25} + C_{27} + C_{29} + C_{31})/(C_{26} + C_{28} + C_{30} + C_{32})]$.

[b] $OEP_{27}=(C_{27}+6C_{29} + C_{31})/4(C_{28} + C_{30})$.

[c] $ACL = [25(C_{25})+27(C_{27})+29(C_{29})+31(C_{31})+33(C_{33})]/(C_{25} + C_{27} + C_{29} + C_{31} + C_{33})$.

carbon preference index ($CPI_{25\text{-}31}$: 3.33–6.49, average: 5.32; $OEP_{27}$: 3.80–6.25, average: 5.22) (**Table 2**), typical of a terrestrial leaf wax and higher plant source. This strong odd-over-even predominance indicates that the source of the *n*-alkanes in the sediments was terrestrial higher plants. On the other hand, the CPI values seem to be related to elevation. For instance, with the exception of sample GGS-7 (6,100 m), the CPI values from low elevation samples were higher than those samples from a high elevation. These results showed that the whole slope of Gongga Mountain was dominated by higher plants and with microbial footprints (Howard et al., 2018). Furthermore, as seen in **Table 2**, CPI values for samples from lower altitudes below 6,000 m ranged from 4.23 to 6.49 with an average of 5.56, indicating that n-alkanes are more often synthesized by higher plants, while CPI values for samples from higher altitudes above 6,000 m ranged from 3.33 to 5.99 with an average of 4.95, indicating that bacterial fingerprints increase with altitude.

Molecular organic geochemistry has also demonstrated that the $n$-$C_{29}$/$n$-$C_{31}$ ratio of *n*-alkanes is indicative of the relative proportion of woody plants to grassy plants (Meyers 1997; Ficken et al., 2000; Li G. et al., 2018). The $C_{29}$ *n*-alkanes dominate the sediments and have little variability, indicating that trees dominated Gongga Mountain and that the climate was relatively stable. The ratio of the $C_{29}$ *n*-alkane to $C_{31}$ *n*-alkanes for all samples varied between 4.94 and 1.76, with a relatively wide range and smaller values at lower altitudes (**Table 2**), indicating a relatively warm and humid climate at lower altitudes. This is due to the fact that as the ratio of $C_{29}/C_{31}$ becomes smaller, $C_{31}$, which represents grassy plants, gradually increases, indicating that grassy plants multiply vigorously as they prefer a relatively warm and humid climate to grow in. In addition, a high ratio of these alkanes indicates a change from a humid to an arid climate. As shown in **Table 2**, the average ratio of $n$-$C_{29}$/$n$-$C_{31}$ tends to be high ($3.6 > 1$) for all samples, indicating that the deposition of the top section between approximately 4,600 m to

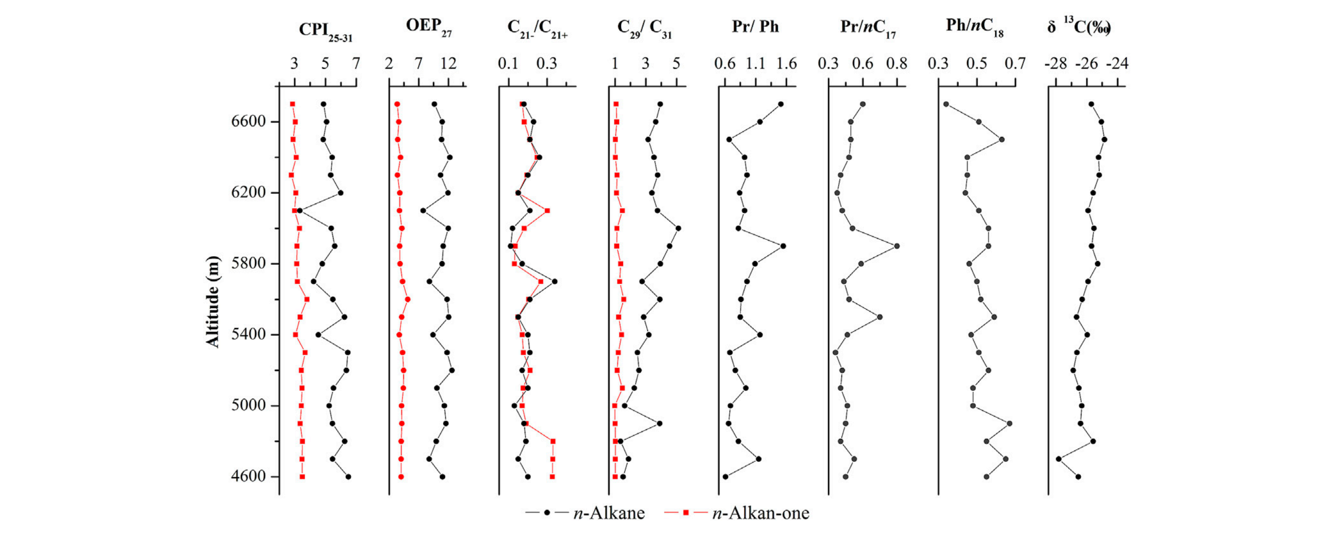


**FIGURE 4 |** Variation of $CPI_{25-31}$, $OEP_{27}$, $C_{21-}/C_{21+}$, $C_{29}/C_{31}$, Pr/Ph, Pr/$nC_{17}$, Ph/$nC_{18}$, and $\delta^{13}C$ of *n*-alkane and *n*-alkan-2-one in the studied samples.

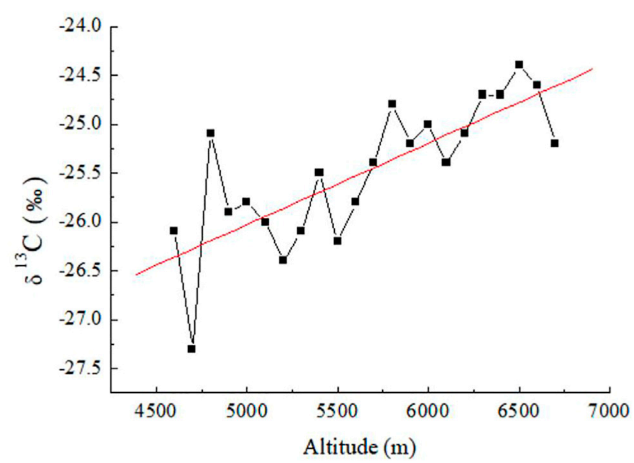


**FIGURE 5 |** Plot of $\delta^{13}C$ versus altitude for the analyzed sediment samples from Gongga Mountain in the Sichuan Basin.

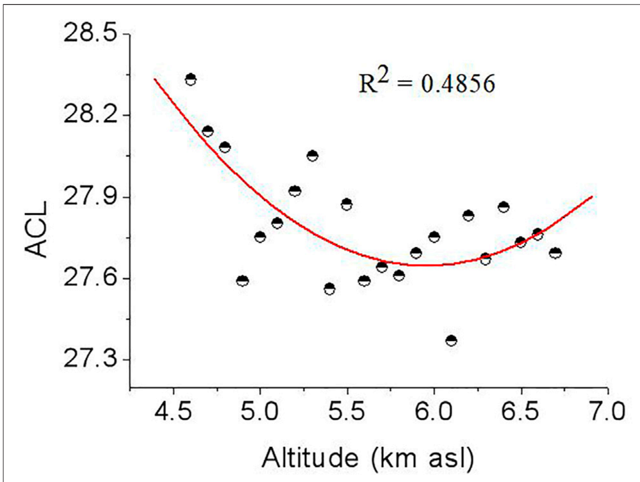


**FIGURE 6 |** Altitudinal variations of $ACL_{27–31}$. $ACL_{27–31}$ is calculated from weighted-mean chain length of $C_{25}$, $C_{27}$, $C_{29}$, $C_{31}$ and $C_{33}$ *n*-alkanes.

6,700 m occurred under relatively continuous humid climate conditions.

Another useful parameter from the *n*-alkane distribution is the average chain length (ACL), which has been suggested to change with plant types. Woody plants display *n*-alkane distributions dominated by the $C_{27}$ or $C_{29}$ *n*-alkanes, whereas grasses have distributions dominated by the $C_{31}$ *n*-alkane (Gamarra and Kahmen 2015; Li et al., 2016). The average ACL is 29.5 for grass, 28.4 for reeds and 27.9 for tree leaves (Duan and Xu 2012). Therefore, grasses usually have high ACL values relatively to those of trees. In our results, samples from elevations of 4,600, 4,700, 4,800, and 5,300 m had ACL values of 28.33, 28.14, 28.08 and 28.05, respectively, while samples from 4,900 m to 6,700 m had ACL values from 27.37 to 27.87 (**Table 2** and **Figure 6**), which are in the range of tree leaves (Duan and Xu, 2012), indicating that woody plants were the main vegetation. In addition, a plot of $ACL_{27-31}$ vs. altitude (**Figure 6**) showed that a quadratic relationship exists between these two variables, with lower $ACL_{27-31}$ values occurring at mid altitudes and higher values occurring at low and high altitudes. The *n*-alkane $ACL_{27-31}$ values reach a minimum in samples from 6,100 m, and the intermittent decrease in ACL in samples from 6,100 m may indicate a temporal increase in merged $C_4$ plants. These results also suggest that the region underwent a relatively cold and wet climate because plants in colder/wetter areas have lower $ACL_{27-31}$ values than those in warmer/drier areas (Zhou et al., 2005; Bush and Mclnerney 2013). Furthermore, the *n*-alkane mean chain length $ACL_{27-31}$ ratio gradually decreased and the *n*-alkane ($C_{29}/C_{31}$) ratio gradually increased as altitude increased from 4,600 m to 6,100 m ($ACL_{27-}$

$_{33}$: 27.37–28.33, average: 27.79 and $C_{29}/C_{31}$: 1.76–5.52, average: 3.54) (**Table 2** and **Figure 6**), indicating an increase in woody plants, which produce a large proportion of the $C_{27}$ and $C_{29}$ *n*-alkanes. This pattern can be best explained in terms of vegetation; that is, woody plants dominate the paleosols, and grasses have less influences, especially near 6,000 m. The increase in the $C_{29}/C_{31}$ ratio from 4.94 to 5.52 with some oscillations in samples from 5,900 to 6,000 m is possibly caused by a decrease in grasses, which produce large proportions of the $C_{29}$ *n*-alkane (Zhou et al., 2005). In contrast, the $C_{29}$ *n*-alkanes dominate the sediments from 5,900 to 6,000 m and biomarkers vary with relatively greater amplitudes and at a higher frequency, indicating that woody plants were dominant and that relatively wetter conditions prevailed during these altitudes. This results in a slightly different conclusion than those drawn from other parameters: i.e., the climate became wetter and colder at 6,100 m. The explanation for this discrepancy needs to be further explored.

## Distribution Characteristics and Possible Source of *n*-Alkan-2-ones

*n*-Alkan-2-ones are commonly observed lipid components of sediments from Gongga Mountain. In all samples, the *n*-alkan-2-ones range from $C_9$ to $C_{33}$ and have a bimodal distribution (**Figure 3**). Lower-molecular-weight (LMW) *n*-alkan-2-ones ($C_9$-$C_{21}$), which reach maximum values at *n*-$C_{17}$ or *i*-$C_{18}$, dominant samples from 4,600 m to 6,700 m, while higher-molecular-weight (HMW) *n*-alkan-2-ones ($C_{23}$-$C_{33}$), with a mode at $C_{27}$ or $C_{29}$, dominate in all samples. Their $\sum n$-$C_{21-}/\sum n$-$C_{21+}$ ratios and the carbon preference indices of the HMW ($C_{23}$-$C_{33}$) *n*-alkan-2-ones (CPI) sensitively reflect the variations in the sediment ecosystem response, also indicating that the organic matter in this sediment was derived from terrestrial herbaceous plants, but was probably reworked by bacteria.

In some studies, *n*-alkan-2-ones that have a close resemblance to the terrigenous *n*-alkane distributions have led several authors to propose that microbial oxidation of *n*-alkanes is the source of *n*-alkan-2-ones, with $\beta$-oxidation of fatty acids followed by decarboxylation as an alternate pathway (Volkman et al., 1981; Albaiges, Algaba, and Grimalt 1984; Lehtonen and Ketola 1990; Nichls and Huang 2007). In Gongga Mountain sediment samples, the *n*-alkan-2-one distribution appears to result from the mixing of two populations of compounds: the long chain components ($C_{23}$-$C_{33}$), which have a strong OEP, and the short chain components ($C_9$-$C_{22}$), which have no OEP (**Table 2** and **Figure 3**). The distribution of *n*-alkanes in all samples is analogous to that of the *n*-alkan-2-ones (**Figure 2** and **Figure 3**), with a long-chain alkane OEP and a short-chain alkane with no OEP, indicating that *n*-alkan-2-ones originated from microbiological subterminal oxidation of *n*-alkanes (Cranwell, Eglinton, and Robinson 1987; Lehtonen and Ketola 1990). The dominance of the $C_{29}$ homologue in both the HMW *n*-alkanes and the *n*-alkan-2-ones throughout the sediments suggests that the oxidation of *n*-alkanes is the favorable pathway (Chen et al., 2019).

Furthermore, the $C_{29}/C_{31}$ and $C_{21}$-/$C_{21+}$ ratio curves of *n*-alkanes and *n*-alkan-2-ones essentially parallel each other, with higher values present in samples from 5,700 m to 6,100 m, suggesting the *n*-alkan-2-ones may be formed from the microbial oxidation of the corresponding *n*-alkanes, as previously proposed (Albaiges, Algaba, and Grimalt 1984; Nichls and Huang. 2007; Wu et al., 2012).

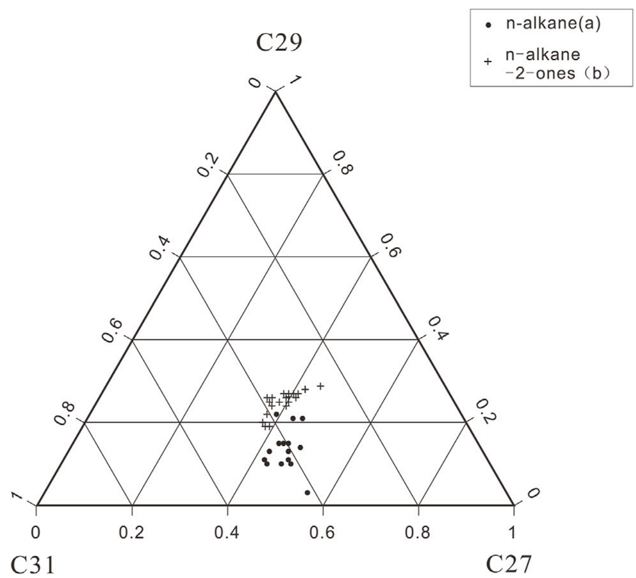


**FIGURE 7 |** Ternary diagram for $C_{27}$, $C_{29}$ and $C_{31}$ *n*-alkane and *n*-alkan-2-one in the studied samples.

In addition, **Figure 7** shows a ternary diagram for the same three *n*-alkanes and *n*-alkan-2-ones ($C_{27}$, $C_{29}$ and $C_{31}$) from the eastern slope of Gongga Mountain; there are two recognizable clusters in these samples. The *n*-alkanes cluster plots are close to the region that characterizes wood plants. However, the *n*-alkan-2-ones cluster plot near the position characterized by grasslands. This difference can best be explained in terms of vegetation; that is, trees dominate the components of the sediment samples, with some increase in the contribution of grasses during the warm stages.

## CONCLUSION

The *n*-alkanes and *n*-alkan-2-ones were analyzed in sediment samples from Gongga Mountain, Sichuan Basin, on the southeastern edge of the Tibetan Plateau, southwest China. The *n*-alkanes and *n*-alkan-2-ones were from a mixed source of bacteria, algae and terrestrial higher plants, and were mainly derived from terrestrial higher plants.

The $C_9$-$C_{21}$/$C_{23}$-$C_{33}$ ratios and the carbon preference indices of the HMW ($C_{23}$-$C_{33}$) n-alkan-2-ones (CPI) of the samples sensitively reflect the variation in the sediment ecosystem's response to climate. The CPI and ACL values of *n*-alkanes in sediments from low latitudes were higher than those from high latitudes. The CPI and ACL values for different climate zones can also indicate the variation in the sediment ecosystem's response to climate.

The stable carbon ($\delta^{13}C$) analyses of the sediments showed that the biomes in the study area were dominated by $C_3$ plants through paleosol cycles and cold and dry climatic conditions existed in the past.

## DATA AVAILABILITY STATEMENT

The original contributions presented in the study are included in the article/Supplementary material, further inquiries can be directed to the corresponding author.

## AUTHOR CONTRIBUTIONS

YW, ZC, and TW contributed ideas and design to the study and engaged in charting. YL and RM performed samples analysis and data processing. YW and TW wrote the first draft of the manuscript.

## FUNDING

Financial support from the National Natural Science Foundation of China (Grant Nos. 42072180; 41772147; 41872146; 41272147) and the Chinese Academy of Sciences Instrument Equipment Function Development Technology Innovation Project (Grant No. E0280101).

## ACKNOWLEDGMENTS

We are also particularly grateful to the reviewers for their constructive comments for the manuscript.

## REFERENCES

Al-Aklabi, A., Al-Khulaidi, A. W., Hussain, A., Al-Sagheer, N., and Al-Sagheer, N. (2016). Main Vegetation Types and Plant Species Diversity along an Altitudinal Gradient of Al Baha Region, Saudi Arabia. *Saudi J. Biol. Sci.* 23, 687–697. doi:10.1016/j.sjbs.2016.02.007

Albaigés, J., Algaba, J., and Grimalt, J. (1984). Extractable and Bound Neutral Lipids in Some Lacustrine Sediments. *Org. Geochem.* 6, 223–236. doi:10.1016/0146-6380(84)90044-5

Andreou, G., and Rapsomanikis, S. (2009). Origins of N-Alkanes, Carbonyl Compounds and Molecular Biomarkers in Atmospheric Fine and Coarse Particles of Athens, Greece. *Sci. Total Environ.* 407, 5750–5760. doi:10.1016/j.scitotenv.2009.07.019

Badewien, T., Vogts, A., and Rullkötter, J. (2015). n-Alkane Distribution and Carbon Stable Isotope Composition in Leaf Waxes of C3 and C4 Plants from Angola. *Org. Geochem.* 89-90, 71–79. doi:10.1016/j.orggeochem.2015.09.002

Bai, Y., Chen, Q., Zhou, Y., Fang, X., and Liu, X. (2020). Terpenoids in Surface Soils from Different Ecosystems on the Tibetan Plateau. *Org. Geochem.* 150, 104125. doi:10.1016/j.orggeochem.2020.104125

Bai, Y., Fang, X., Gleixner, G., and Mügler, I. (2011). Effect of Precipitation Regime on δD Values of Soil N-Alkanes from Elevation Gradients - Implications for the Study of Paleo-Elevation. *Org. Geochem.* 42, 838–845. doi:10.1016/j.orggeochem.2011.03.019

Banerjee, A., Sinha, A. K., Jain, A. K., Thomas, N. J., Misra, K. N., and Chandra, K. (1998). A Mathematical Representation of Rock-Eval Hydrogen Index vs Tmax Profiles. *Org. Geochem.* 28, 43–55. doi:10.1016/S0146-6380(97)00119-8

Behar, F., Beaumont, V., and De B. Penteado, H. L. (2001). Rock-Eval 6 Technology: Performances and Developments. *Oil Gas Sci. Technol. - Rev. IFP* 56, 111–134. doi:10.2516/ogst:2001013

Bezabih, M., Pellikaan, W. F., Tolera, A., and Hendriks, W. H. (2011). Evaluation of N-Alkanes and Their Carbon Isotope Enrichments (δ13C) as Diet Composition Markers. *Animal* 5 (1), 57–66. doi:10.1017/S1751731110001515

Bi, X., Sheng, G., Liu, X., Li, C., and Fu, J. (2005). Molecular and Carbon and Hydrogen Isotopic Composition of N-Alkanes in Plant Leaf Waxes. *Org. Geochem.* 36, 1405–1417. doi:10.1016/j.orggeochem.2005.06.001

Bray, E. E., and Evans, E. D. (1961). Distribution of N-Paraffins as a Clue to Recognition of Source Beds. *Geochimica Cosmochimica Acta* 22, 2–15. doi:10.1016/0016-7037(61)90069-2

Bush, R. T., and McInerney, F. A. (2015). Influence of Temperature and C 4 Abundance on N -alkane Chain Length Distributions across the Central USA. *Org. Geochem.* 79, 65–73. doi:10.1016/j.orggeochem.2014.12.003

Bush, R. T., and McInerney, F. A. (2013). Leaf Wax N-Alkane Distributions in and across Modern Plants: Implications for Paleoecology and Chemotaxonomy. *Geochimica Cosmochimica Acta* 117, 161–179. doi:10.1016/j.gca.2013.04.016

Carvajal-Ortiz, H., and Gentzis, T. (2015). Critical Considerations when Assessing Hydrocarbon Plays Using Rock-Eval Pyrolysis and Organic Petrology Data: Data Quality Revisited. *Int. J. Coal Geol.* 152, 113–122. doi:10.1016/j.coal.2015.06.001

Cayet, C., and Lichtfouse, E. (2001). δ13C of Plant-Derived N-Alkanes in Soil Particle-Size Fractions. *Org. Geochem.* 32, 253–258. doi:10.1016/s0146-6380(00)00172-8

Chen, L., Zhou, W., Zhang, Y., Zheng, Y., and Huang, X. (2020). Postglacial Floral and Climate Changes in Southeastern China Recorded by Distributions of N-Alkan-2-Ones in the Dahu Sediment-Peat Sequence. *Palaeogeogr. Palaeoclimatol. Palaeoecol.* 538, 109448. doi:10.1016/j.palaeo.2019.109448

Chen, Z., Liu, X., Guo, Q., Jiang, C., and Mort, A. (2017). Inversion of Source Rock Hydrocarbon Generation Kinetics from Rock-Eval Data. *Fuel* 194, 91–101. doi:10.1016/j.fuel.2016.12.052

Cheshire, S., Craddock, P. R., Xu, G., Sauerer, B., Pomerantz, A. E., McCormick, D., et al. (2017). Assessing Thermal Maturity beyond the Reaches of Vitrinite Reflectance and Rock-Eval Pyrolysis: A Case Study from the Silurian Qusaiba Formation. *Int. J. Coal Geol.* 180, 29–45. doi:10.1016/j.coal.2017.07.006

Collister, J. W., Rieley, G., Stern, B., Eglinton, G., and Fry, B. (1994). Compound-specific δ 13C Analyses of Leaf Lipids from Plants with Differing Carbon Dioxide Metabolisms. *Org. Geochem.* 21, 619–627. doi:10.1016/0146-6380(94)90008-6

Coplen, T. B., Brand, W. A., Gehre, M., Gröning, M., Meijer, H. A. J., Toman, B., et al. (2006). New Guidelines for δ13C Measurements. *Anal. Chem.* 78 (7), 2439–2441. doi:10.1021/ac052027c

Cortina, A., Grimalt, J. O., Rigual-Hernández, A., Ballegeer, A.-M., Martrat, B., Sierro, F. J., et al. (2016). The Impact of Ice-Sheet Dynamics in Western Mediterranean Environmental Conditions during Terminations. An Approach Based on Terrestrial Long Chain N-Alkanes Deposited in the Upper Slope of the Gulf of Lions. *Chem. Geol.* 430, 21–33. doi:10.1016/j.chemgeo.2016.03.015

Cranwell, P. A., Eglinton, G., and Robinson, N. (1987). Lipids of Aquatic Organisms as Potential Contributors to Lacustrine Sediments-II. *Org. Geochem.* 11, 513–527. doi:10.1016/0146-6380(87)90007-6

Crausbay, S., Genderjahn, S., Hotchkiss, S., Sachse, D., Kahmen, A., and Arndt, S. K. (2014). Vegetation Dynamics at the Upper Reaches of a Tropical Montane Forest Are Driven by Disturbance over the Past 7300 Years. *Arct. Antarct. Alp. Res.* 46, 787–799. doi:10.1657/1938-4246-46.4.787

Deines, P. (1980). "The Isotopic Composition of Reduced Organic Carbon," in *Handbook of Environmental Isotopic GeochemistryThe Terrestrial Environment*. Editors P. Fritz and J. C. Fontes (Amsterdam: Elsevier), Vol. 1, 329–406. doi:10.1016/B978-0-444-41780-0.50015-8

Demaison, G., and Huizinga, B. J. (1994). "Genetic Classification of Petroleum Systems Using Three Factors: Charge, Migration Entrapment," in *The Petroleum Systems: From Source to Trap*. Editors L. B. Magoon and W. G. Dow (Tulsa: AAPG Memoir), 60, 73–80. doi:10.1002/dev.21263

Didyk, B. M., Simoneit, B. R. T., Brassell, S. C., and Eglinton, G. (1978). Organic Geochemical Indicators of Palaeoenvironmental Conditions of Sedimentation. *Nature* 272, 216–222. doi:10.1038/272216a0

Duan, Y., and Xu, L. (2012). Distributions of N-Alkanes and Their Hydrogen Isotopic Composition in Plants from Lake Qinghai (China) and the Surrounding Area. *Appl. Geochem.* 27, 806–814. doi:10.1016/j.apgeochem.2011.12.008

Eglinton, G., and Hamilton, R. J. (1967). Leaf Epicuticular Waxes. *Science* 156, 1322–1335. doi:10.1126/science.156.3780.1322

Fang, J., Wu, F., Xiong, Y., Li, F., Du, X., An, D., et al. (2014). Source Characterization of Sedimentary Organic Matter Using Molecular and Stable Carbon Isotopic Composition of N-Alkanes and Fatty Acids in Sediment Core from Lake Dianchi, China. *Sci. Total Environ.* 473-474, 410–421. doi:10.1016/j.scitotenv.2013.10.066

Farquhar, G. D., Ehleringer, J. R., and Hubick, K. T. (1989). Carbon Isotope Discrimination and Photosynthesis. *Annu. Rev. Plant. Physiol. Plant. Mol. Biol.* 40, 503–537. doi:10.1146/annurev.pp.40.060189.002443

Ficken, K. J., Li, B., Swain, D. L., and Eglinton, G. (2000). An N-Alkane Proxy for the Sedimentary Input of Submerged/floating Freshwater Aquatic Macrophytes. *Org. Geochem.* 31, 745–749. doi:10.1016/s0146-6380(00)00081-4

France-Lanord, C., and Derry, L. A. (1994). δC of Organic Carbon in the Bengal Fan: Source Evolution and Transport of C3 and C4 Plant Carbon to Marine Sediments. *Geochimica Cosmochimica Acta* 58 (21), 4809–4814. doi:10.1016/0016-7037(94)90210-0

Gamarra, B., and Kahmen, A. (2015). Concentrations and δ2H Values of Cuticular N-Alkanes Vary Significantly Among Plant Organs, Species and Habitats in Grasses from an Alpine and a Temperate European Grassland. *Oecologia* 178, 981–998. doi:10.1007/s00442-015-3278-6

George, S. C., and Jardine, D. R. (1994). Ketones in a Proterozoic Dolerite Sill. *Org. Geochem.* 21, 829–839. doi:10.1016/0146-6380(94)90042-6

Howard, S., McInerney, F. A., Hall, P. A., and Andrae, P. A. (2018). Modelling Leaf Wax N -alkane Inputs to Soils along a Latitudinal Transect across Australia, *Org. Geochem.* 121. 126–137, doi:10.1016/j.orggeochem.2018.03.013

Hughes, W. B., Holba, A. G., and Dzou, L. I. P. (1995). The Ratios of Dibenzothiophene to Phenanthrene and Pristane to Phytane as Indicators of Depositional Environment and Lithology of Petroleum Source Rocks. *Geochimica Cosmochimica Acta* 59, 3581–3598. doi:10.1016/0016-7037(95)00225-o

Jackson, L. L., and Roof, S. R. (1992). Determination of the Forms of Carbon in Geologic Materials. *Geostand. Newsl.* 16, 317–323. doi:10.1111/j.1751-908X.1992.tb00495.x

Jansen, B., Haussmann, N. S., Tonneijck, F. H., Verstraten, J. M., and de Voogt, P. (2008). Characteristic Straight-Chain Lipid Ratios as a Quick Method to Assess Past Forest-Páramo Transitions in the Ecuadorian Andes. *Palaeogeogr. Palaeoclimatol. Palaeoecol.* 262, 129–139. doi:10.1016/j.palaeo.2008.02.007

Jia, G., Wei, K., Chen, F., and Peng, P. a. (2008). Soil N-Alkane δD vs. Altitude Gradients along Mount Gongga, China. *Geochimica Cosmochimica Acta* 72 (21), 5165–5174. doi:10.1016/j.gca.2008.08.004

Lehtonen, K., and Ketola, M. (1990). Occurrence of Long-Chain Acyclic Methyl Ketones in Sphagnum and Carex Peats of Various Degress of Humification. *Org. Geochem.* 15, 275–280. doi:10.1016/0146-6380(90)90005-K

Li, G., Li, L., Tarozo, R., Longo, W. M., Wang, K. J., Dong, H., et al. (2018a). Microbial Production of Long-Chain N-Alkanes: Implication for Interpreting Sedimentary Leaf Wax Signals. *Org. Geochem.* 115, 24–31. doi:10.1016/j.orggeochem.2017.10.005

Li, M., ChenCao, Z. T. T., Cao, T., Ma, X., Liu, X., Li, Z., et al. (2018). Expelled Oils and Their Impacts on Rock-Eval Data Interpretation, Eocene Qianjiang Formation in Jianghan Basin, China. *Int. J. Coal Geol.* 191, 37–48. doi:10.1016/j.coal.2018.03.001

Li, Y. Y., Yang, S. L., Wang, X., Hu, J. F., Cui, L. L., Huang, X. F., et al. (2016). Leaf Wax N-Alkane Distributions in Chinese Loess since the Last Glacial Maximum and Implications for Paleoclimate. *Quat. Int.* 399, 190–197. doi:10.1016/j.quaint.2015.04.029

Lichtfous, R., Derenne, S., Mariotti, A., and Largeau, C. (1994). Possible Algal Origin of Long Chain Odd N-Alkanes in Immature Sediments as Revealed by Distributions and Carbon Isotope Ratios. *Org. Geochem.* 22, 1023–1027. doi:10.1016/0146-6380(94)90035-3

Lim, J., Nahm, W. H., Kim, J. K., and Yang, D. Y. (2010). Regional Climate-Driven $C_3$ and $C_4$ Plant Variation in the Cheollipo Area, Korea, during the Late Pleistocene. *Palaeogeogrphy Palaeoclimatol. Palaeoecol.* 298, 370–377. doi:10.1016/j.palaeo.2010.10.021

Liu, W. G., Huang, Y. S., An, Z. S., Clemens, S. C., Li, L., Prell, W. L., et al. (2005). Summer Monsoon Intensity Controls $C_4$/$C_3$ Plant Abundance during the Last 35 Ka in the Chinese Loess Plateau: Carbon Isotope Evidence from Bulk Organic Matter and Individual Leaf Waxes. *Palaeogeogrphy Palaeoclimatol. Palaeoecol.* 220, 243–254. doi:10.1016/j.palaeo.2005.01.001

Luo, J., Tang, R. G., Sun, S. Q., Yang, D. D., She, J., and Yang, P. J. (2015). Lead Distribution and Possible Sources along Vertical Zonespectrum of Typical Ecosystems in the Gongga Mountain, Eastern Tibetan Plateau. *Atmos. Environ.* 115, 132–140. doi:10.1016/j.atmosenv.2015.05.022

Meyers, P. A. (1997). Organic Geochemical Proxies of Paleoceanographic, Paleolimnologic, and Paleoclimatic Processes. *Org. Geochem.* 27, 213–250. doi:10.1016/S0146-6380(97)00049-1

Mille, G., Asia, L., Guiliano, M., Malleret, L., and Doumenq, P. (2007). Hydrocarbons in Coastal Sediments from the Mediterranean Sea (Gulf of Fos Area, France). *Mar. Pollut. Bull.* 54, 566–575. doi:10.1016/j.marpolbul.2006.12.009

Nichols, J. E., and Huang, Y. S. (2007). C23-C31 N-Alkan-2-Ones Are Biomarkers for the Genus Sphagnum in Foreshwater Peatlands. *Org. Geochem.* 38, 1972–1976. doi:10.1016/j.orggeochem.2007.07.002

Peters, K. E. (1986). Guidelines for Evaluating Petroleum Source Rock Using Programmed Pyrolysis. *AAPG Bull.* 70, 318–329. doi:10.1306/94885688-1704-11d7-8645000102c1865d

Peters, K. E., and Moldowan, J. M. (1993). The Biomarker Guide, Interpreting Molecular Fossils in Petroleum and Ancient Sediments. *Choice Rev. Online* 30, 2690. doi:10.5860/choice.30-2690

Poynter, J., and Eglinton, G. (1991). The Biomarker Concept-Strengths and Weaknesses. *Fresenius' J. Anal. Chem.* 339, 725–731. doi:10.1007/BF00321733

Robison, C. R. (1997). Hydrocarbon Source Rock Variability within the Austin Chalk and Eagle Ford Shale (Upper Cretaceous), East Texas, U.S.A. *Int. J. Coal Geol.* 34, 287–305. doi:10.1016/s0166-5162(97)00027-x

Rontani, J., Bonin, P., Vaultier, F., Guasco, S., and Volkman, J. K. (2013). Anaerobic Bacterial Degradation of Pristenes and Phytenes Inmarine Sediments Does Not Lead to Pristane and Phytane during Early Diagenesis. *Org. Geochem.* 58, 43–55. doi:10.1016/j.orggeochem.2013.02.001

Routh, J., Hugelius, G., Kuhry, P., Filley, T., Tillman, P. K., Becher, M., et al. (2014). Multiproxy Study of Soil Organic Matter Dynamics in Permafrost Peat Deposits Reveal Vulnerability to Climate Change in the European Russian Arctic. *Chem. Geol.* 368, 104–117. doi:10.1016/j.chemgeo.2013.12.022

Sukumar, R., Ramesh, R., Pant, R. K., and Rajagopalan, G. (1993). A δ13C Record of Late Quaternary Climate Change from Tropical Peats in Southern India. *Nature* 364. 703–705. doi:10.1038/364703a0

Sun, J. M., Lv, T. Y., Zhang, Z. Q., Wang, X., and Liu, W. G. (2012). Stepwise Expansions of $C_4$ Biomass and Enhanced Seasonal Precipitation and Regional Aridity during the Quaternary on the Southern Chinese Loess Plateau. *Quat. Sci. Rev.* 34, 57–65. doi:10.1016/j.quascirev.2011.12.007

Thomas, A. (1999). Overview of the Geoecology of the Gongga Shan Range, Sichuan Province, China. *Mt. Res. Dev.* 19, 17–30. doi:10.2307/3674110

Thomas, A. (1997). The Climate of the Gongga Shan Range, Sichuan Province, PR China. *Arct. Alp. Res.* 29, 226–232. doi:10.2307/1552051

Vogts, A., Moossen, H., Rommerskirchen, F., and Rullktter, J. (2009). Distribution Patterns and Stable Carbon Isotopic Composition of Alkanes and Alkan-1-Ols from Plant Waxes of African Rain Forest and Savanna $C_3$ Species. *Org. Geochem.* 40, 1037–1054. doi:10.1016/j.orggeochem.2009.07.011

Volkman, J. K., Gillan, F. T., Johns, R. B., and Eglinton, G. (1981). Source of Neutral Lipids in a Temperate Intertidal Sediment. *Geochimica Cosmochimica Acta* 45, 1817–1828. doi:10.1016/0016-7037(81)90012-0

Wang, N., Zong, Y. Q., Brodie, C. R., and Zheng, Z. (2014). An Examination of the Fidelity of N-Alkanes as a Palaeoclimate Proxy from Sediments of Palaeolake Tianyang, South China. *Quat. Int.* 333, 100–109. doi:10.1016/j.quaint.2014.01.044

Wang, Y. L., Fang, X. M., Zhang, T. W., Li, Y. M., Wu, Y. Q., He, D. X., et al. (2010). Predominance of Even Carbon-Numbered N-Alkanes from Lacustrine Sediments in Linxia Basin, NE Tibetan Plateau: Implications for Climate Change. *Appl. Geochem.* 25, 1478–1486. doi:10.1016/j.apgeochem.2010.07.002

Wei, J., Liu, W. G., Cheng, J. M., and Li, W. J. (2015). $\delta^{13}C$ Values of Plants as Indicators of Soil Water Content in Modern Ecosystems of the Chinese Loess Plateau. *Ecol. Eng.* 77, 51–59. doi:10.1016/j.ecoleng.2015.01.012

Wu, Y. q., Wang, Y. l., Lei, T. Z., Chang, J., and Xia, Y. Q. (2012). Possible Origin of High Molecular Weight *N*-Alkan-2-Ones in Jurassic Bitumens from the Sichuan Basin in Southwest China. *Chem. Technol. Fuels Oils* 48, 195–201. doi:10.1007/s10553-012-0358-8

Wu, Y. q., Xia, Y. Q., Wang, Y. l., Lei, T. Z., Liu, Y., Liu, Y. H., et al. (2016). The Geochemical Characteristics of Coals from the Junggar Basin in Northwest China and the Relation of the Configuration of Pristane with Maturity in Highly Mature and Over-mature Samples. *Oil Gas Sci. Technol.* 71, 1–11. doi:10.2516/ogst/2015026

Xue, J. B., Zhong, W., and Cao, J. Y. (2014). Changes in $C_3$ and $C_4$ Plant Abundances Reflect Climate Changes from 41,000 to 10,000 Yr Ago in Northern Leizhou Peninsula, South China. *Palaeogeogrphy Palaeoclimatol. Palaeoecol.* 396, 173–182. doi:10.1016/j.palaeo.2014.01.003

Yang, S. L. (2012). Warm-season Precipitation as the Dominant Control on $C_3/C_4$ Plant Variations in Northern china: Evidence from Carbon and Oxygen Isotope Composition of Pedogenic Carbonate. *Quat. Int.* 279-280, 546. doi:10.1016/j.quaint.2012.08.1919

Zhong, X. H., Zhang, W. J., and Luo, J. (1999). The Characteristics of the Mountain Ecosystem and Environment in the Gongga Mountain Region. *Ambio* 28, 648–654. CNKI:SUN:RLHJ.0.1999-08-003.

Zhou, W. J., Xie, S. C., Meyers, P. A., and Zheng, Y. H. (2005). Reconstruction of Late Glacial and Holocene Climate Evolution in Southern China from Geolipids and Pollen in the Dingnan Peat Sequence. *OrganicGeochemistry* 36, 1272–1284. doi:10.1016/j.orggeochem.2005.04.005

**Conflict of Interest:** The authors declare that the research was conducted in the absence of any commercial or financial relationships that could be construed as a potential conflict of interest.

**Publisher's Note:** All claims expressed in this article are solely those of the authors and do not necessarily represent those of their affiliated organizations, or those of the publisher, the editors and the reviewers. Any product that may be evaluated in this article, or claim that may be made by its manufacturer, is not guaranteed or endorsed by the publisher.